

Study of Intra organelle Nanoporation of Multilayer Dense Osteoblast Cell

S. Sarkar
 A E I, SMIT, Sikkim, India

R Mahapatra
 ECE, NIT, Durgapur, India

M.K.Ghose
 CSE, SMIT, Sikkim, India

ABSTRACT

This research paper represents the theoretical and experimental study of intra organelle nano poration of multi layer osteoblast cell .It is observed that the Pico pulse has the remarkable response for nano pores generation on the intra organelle and chemicals are entered into the cell. The reported study encourage that the efficiency of nanoporation can be control by the specification of micro chip. It is also exposed that the key parameter of nanoporation such as intra organelle voltage, pore radius, pore density, pressure, surface tension and ion uptake are externally controlled by user defined hybrid 3D micro chip.

Keywords

Picoseconds Pulsed Electric Field (psPEF), bio Micro chip, Dense Osteoblast cell, Intra- organelle, nanoporation.

1. INTRODUCTION

Due to the typical morphological structure, the osteoblast cell is more rigid than other biological cell. This structure gives a challenge to the scientist for its picoporation and its membrane and intra organelle characterizations. Although some experiment and theoretical approach have been performed on outer membrane but the pore formation in intra organelle concept is till now limited. In our study we have tried to overcome the restrictions and observed that when the pico pulse is applied nano pores are generated on the intra organelle of the dense multi layer osteoblast cell. In drug delivery system the pico poration of the intra organelle plays an important role to introduced the drugs into the osteoblast cell. Previously some work has been done considering the single layer structure of osteoblast cell which gives the limiting information about the cell electroporation. We are focusing on that limitation and consider the original bi-layer structure of osteoblast cell. In our study we observed that the pico pulse has a remarkable response on intra cellular pore generation having the pore radius of 10^{-10} m level if the rigid cell is placed into a specially design micro chip where shape of micro fluidic channel and micro electrode are hybrid in nature and electrodes are bi metallic[1]-[8].

In recent developments of micro technologies and micro fluidics techniques permit consideration of the design and fabrication of new innovative tools for biology. The main benefits of these technologies consist in their miniaturization and parallelization capabilities, as well as real-time observation in the case where transparent materials are used for the device fabrication [9], [10].

But till now the information regarding the effect of Pico pulse on intra cellular organism of dense rigid cell like osteoblast cell are limited. However, the delivery of the psPEF to the cells without deformation of biological contents requires a specific design. In this context, the work presented in this paper describes the design, fabrication and characterization of a hybrid micro chip

device specifically optimized for ps PEF exposure of intra organelle picoporation of dense osteoblast cell followed by the development of a micro-fluidic model of the system of our current study. Biological characterizations of the cells exposed on the chip to 10 ps pulsed electric fields using a florescent dye are carried out. The development of such hybrid micro chip has the prime importance to provide the new knowledge on the intra cellular picoporation.

2. ANALYTICAL STUDY

2.1 Derivation of the induced intra organelle voltages

C.Yao et al gave the following Schematic diagram of double -shelled spherical cell in suspension, which is used for theoretical explanation of outer and inner membrane potential of a biological cell[11]-[15].

According to the transfer functions defined by C.Yao the inner and outer membranes to a given rectangular pulse electric field $E(s)$ can be obtained

$$Vn(t) = L^{-1}[Hn(S). E (S)] \text{ ----- (1)}$$

$$\& Vm(t) = L^{-1}[Hm(S). E (S)] \text{ (2)}$$

Where,

$$Hm(s) = \frac{Vm(s) \cos \theta}{E(s)} = \frac{1.5Rc \cos \theta}{\tau_{cell} S+1}$$

$$\& Hn(S) = \frac{Vn(S) \cos \theta}{E(S)} = \frac{1.5 \tau_{cell} Rn \cos \theta}{(\tau_{nuc} S+1)+(\tau_{cell} S+1)}$$

After simplification of equation (1) & (2) we get the outer membrane potential ($Vm(t)$) and inner membrane potential $Vn(t)$ are as follows

$$Vm(t) = 1.5 Rc E(t) \left[-e^{-\frac{t}{\tau_{cell}}} - 1(t - \tau) + e^{-\frac{t-\tau}{\tau_{cell}}} \cdot 1(t - \tau) \right] \cos \theta \text{ --- (3)}$$

$$Vn(t) = \frac{1.5 \tau_{cell} Rnuc E(t)}{\tau_{cell} - \tau_{nuc}} \left[\left(e^{-\frac{t}{\tau_{cell}}} - e^{-\frac{t}{\tau_{nuc}}} \right) - \left(e^{-\frac{t-\tau}{\tau_{cell}}} - e^{-\frac{t-\tau}{\tau_{nuc}}} \right) \cdot 1.(t - \tau) \right] \cos \theta \text{ ----- (4)}$$

As we know that $E(t) = v/d$, where v =applied voltage & d = distances in between two electrode. We replace $E(t) = v/d$ in equation (3) & (4) and get outer membrane potential ($Vm(t)$) is

$$Vm(t) = 1.5 Rc \left(\frac{v}{d} \right) \left[-e^{-\frac{t}{\tau_{cell}}} - 1(t - \tau) + e^{-\frac{t-\tau}{\tau_{cell}}} \cdot 1(t - \tau) \right] \cos \theta \text{ --- (5)}$$

& inner membrane is

$$Vn(t) = \frac{1.5 \tau_{cell} Rnuc (v/d)}{\tau_{cell} - \tau_{nuc}} \left[\left(e^{-\frac{t}{\tau_{cell}}} - e^{-\frac{t}{\tau_{nuc}}} \right) - \left(e^{-\frac{t-\tau}{\tau_{cell}}} - e^{-\frac{t-\tau}{\tau_{nuc}}} \right) \cdot 1.(t - \tau) \right] \cos \theta \text{ ---- (5)}$$

According to the frequency response characteristic the inner and outer membrane potential are expressed as follows,

$$Vn(t) = L^{-1}[Hn(S).E(S)] \text{----- (6) \&}$$

$$Vm(t) = L^{-1}[Hm(S).E(S)] \text{----- (7)}$$

After simplification of equation (6) & (7) we get the outer membrane potential ($Vm(t)$) and innermembrane potential $Vn(t)$ are as follows

$$Vm(t) = 1.5 R_c E(t) \left[-e^{-\frac{t}{\tau_{cell}}} - 1(t - \tau) + e^{\frac{t-\tau}{\tau_{cell}}} \cdot 1(t - \tau) \right] \cos \theta \text{----- (8)}$$

$$Vn(t) = \frac{1.5 \tau_{cell} R_{nuc} E(t)}{\tau_{cell} - \tau_{nuc}} \left[\left(e^{-\frac{t}{\tau_{cell}}} - e^{-\frac{t}{\tau_{nuc}}} \right) - \left(e^{-\frac{t-\tau}{\tau_{cell}}} - e^{-\frac{t-\tau}{\tau_{nuc}}} \right) \right] \cos \theta \text{----- (9)}$$

As we know that $E(t) = v/d$, where v =applied voltage & d = distances in between two electrode. We replace $E(t) = v/d$ in equation (8) & (9) and get outer membrane potential ($Vm(t)$) is

$$Vm(t) = 1.5 R_c (v/d) \left[-e^{-\frac{t}{\tau_{cell}}} - 1(t - \tau) + e^{\frac{t-\tau}{\tau_{cell}}} \cdot 1(t - \tau) \right] \cos \theta \text{---- (10)}$$

& inner membrane is

$$Vn(t) = \frac{1.5 \tau_{cell} R_{nuc} (v/d)}{\tau_{cell} - \tau_{nuc}} \left[\left(e^{-\frac{t}{\tau_{cell}}} - e^{-\frac{t}{\tau_{nuc}}} \right) - \left(e^{-\frac{t-\tau}{\tau_{cell}}} - e^{-\frac{t-\tau}{\tau_{nuc}}} \right) \right] \cdot 1. (t - \tau) \cos \theta \text{----- (11)}$$

2.2 Derivation of the radius of nanopores

Based on the theory of membrane permeabilization[21]-[29], nano pores are initially created with a radius of r^* . By increasing the applied electric field, nano pores start to develop in order to minimize the energy of the cell membrane. For the intra organelle with n nanopores, the rate of change of their radius of pore(r), can be determined by the following set of equations:

$$U(r, Vn, Ap) = \frac{D}{KT} \left\{ 4\beta \left(\frac{r^*}{r} \right)^4 \frac{1}{r} - 2\pi\gamma + 2\pi\sigma r + \frac{[\Delta\phi]^2 Fmax}{1+rh/(r+ri)} \right\} \text{-- (12)}$$

Where D is the diffusion co efficient, K = boltz man constant, T =absolute temp, $\phi(r, \theta)$ =intra organelle potential. γ = surface tention. The constants of the above equations are defined in Table 1.

2.3 Calculation of the intra organelle pore current

On the other hand from the some references we have come to know that the outer & inner membrane pore current are expressed respectively [17], [18],

$$I_{epi} = \frac{\pi r m^2 \sigma \Delta\phi}{Fh} * \frac{e^{(\Delta\phi-1)}}{\frac{w_0 * e^{(w_0-nv_n(t))} - n\Delta\phi}{w_0 - nV(t)} * e^{\Delta\phi(t)} - X} \text{-- (13)}$$

$$\text{And } X = \frac{w_0 * e^{(w_0+nvn(t))} + n\Delta\phi}{w_0 + nV(t)} \text{----- (14)}$$

Where I_{epi} Intra organelle pore current.

2.4 Derivation of the intra organelle pressure

From various literature surveys[21],[29], it is come to know that when electric field is applied on a biological cell specific pressure is inserted into the membrane which is mathematically expressed as

$$\& Pi = \frac{\epsilon n \Delta\phi^2}{2h^2} \text{----- (15)}$$

2.5 Derivation of the intra organelle surface tension

As we know when the electric field is applied on the biological cell its molecular & chemical property are changes which may cause the change of surface tension which is mathematically expressed as[19][20].

$$\Gamma_{in} = \frac{2 * \epsilon n * \Delta\phi}{hi} \text{----- (16)}$$

Where Γ_{in} is the surface tension of intra organelle and hi are the thickness of inner membrane.

2.6 Derivation of the intra organelle pore density

DeBruin KA, Krassowska W (1999a) exposed that the rate of creation of nanopores at intra organelle can be found as [21]-[29]

$$\frac{dN(t)}{dt} = \alpha * e^{(\Delta\phi/V_{ep})^2} \left(1 - \frac{N(t)}{N_{eq}(Vn)} \right) \text{----- (17)}$$

Where $N(t)$ is the pore density.

2.7 Derivation of the intra organelle ion uptake

It is known from the bio chemistry that the ion uptake can be calculated by following mathematical calculation [21], [29],

$$I_{uptake} = Kf \left[1 - \left(1 + Kp \cdot te \left(1 + \frac{Kp \cdot te}{2} \right) \right) * e^{-Kp \cdot te} \right] \text{-- (18)}$$

Where $Kf = \frac{D \cdot Sc}{Vc \cdot d}$, and $Kp = e^x$,

$$x = \left[\frac{9 \cdot \Delta R \cdot Vp \cdot a^2 \cdot \epsilon_0 (\epsilon w - \epsilon c)}{8 \cdot Kb \cdot T \cdot d^2} \right] * Vn^2$$

D = Diffusion co efficient,

Vc = Area of the pore, d = thickness. $Sc = N \cdot \pi \cdot r^2$, $\Delta R \cdot Vp = \pi \cdot d(r_1^2 - r^2)$,

T = Temp in kelvin. Kb = Boltz man constant. ϵw = permittivity of water,

ϵc = permittivity of cytoplasm.&
 te = pulse duration. r_1 = radius of pore, r = radius of initial pores,

$V_n = \text{intra organelle potential.}$

3. NUMERICAL SIMULATION

In this study, above Equations are solved numerically to find the electric potential developed in outer and inner membrane to investigate the creation of nano-pores on the cell membrane. The Mat lab 7.2 & Comsol-4.3a, commercial package was used in the numerical simulations. In order to discrete the solution domain, unstructured meshes were applied. The solution domain was broken into small meshes to allow meshes to fully cover the solution domain without overlapping.

4. USED PARAMETER

Table 1 Values for constants and parameters used in the simulations

parameter	Cell parameters	value	Ref no
conductivity (S/m)	Extracellular medium (σ_e)	10×10^{-3}	29
	Cell membrane(σ_m)	1.2×10^{-7}	
	Cell cytoplasm(σ_c)	0.039s	
	Nuclear membrane(σ_n)	10×10^{-1}	
	Nuclear cytoplasm(σ_n)	0.08s	
relative permittivity	Extracellular medium(ϵ_e)	80	
	Cell membrane(ϵ_m)	22	
	Cell cytoplasm(ϵ_c)	93	
	Nuclear membrane(ϵ_n)	22	
	Nuclear cytoplasm(ϵ_n)	93	
Geometry parameter (μm)	Cell radius(r_c)	$12 \mu\text{m}$	
	Cell membrane thickness(d)	$0.006\mu\text{m}$	
	Nuclear radius(r_n)	$6 \mu\text{m}$	
Constant parameters	N_0	$1 * 10^9$	
	D	$5 * 10^{-14}$	
	K	$1.38065 * 10^{-23}$	
	T	300	
	β	$1.4 * 10^{-19}$	
	γ	$1.8 * 10^{-11}$	
	F_{max}	$0.7 * 10^{-9}$	
	σ	$1 * 10^{-6}$	
	rh	$0.97 * 10^{-9}$	
	ri	$0.31 * 10^{-9}$	
	r	$0.7 * 10^{-9}$	
	r_l	$1.2 * 10^{-9}$	

5. MATERIALS AND METHODS

5.1 Design methodology

The biochip is composed of a $100\mu\text{m}$ thick SU8 micro fluidic channel including thick bi metallic electrode (Bi and Au) electrodes with a typical thickness of $50\mu\text{m}$, in which cells suspended in a biological medium are injected. Bi-metallic is chosen as material for the electrodes because of its excellent electrical properties and bio compatibility. The biochip is designed in such a way that the pulsed electric field is absorbed and dissipated mainly in the biological medium placed between the electrodes within which cells to be treated are flowed.

5.2 Design Simulation and Analysis of hybrid micro chip

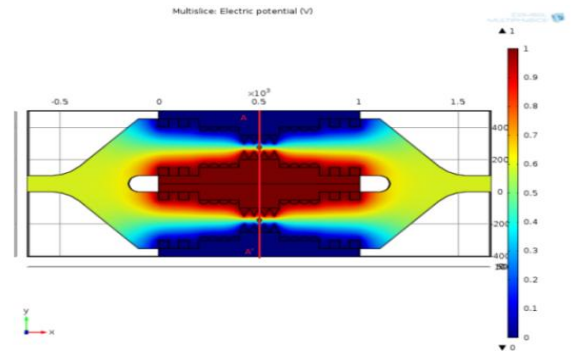


Fig 3 Top view of electrical potential distribution within the 3D hybrid micro chip

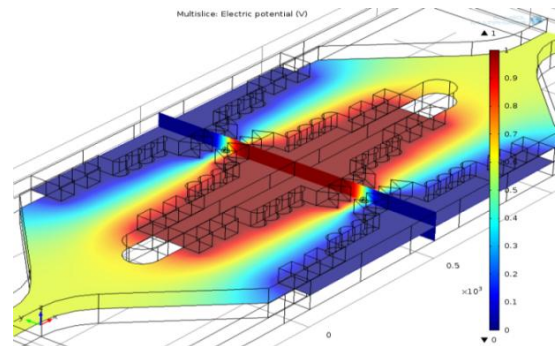


Fig 4 complete electrical potential distribution within the 3D hybrid micro chip

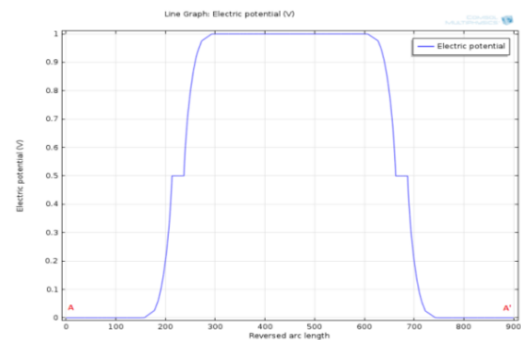


Fig 5 Graphical view of electrical potential distribution with respect to height of the bi metallic electrode within the 3D hybrid micro chip

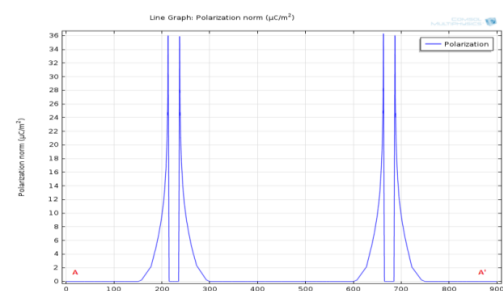


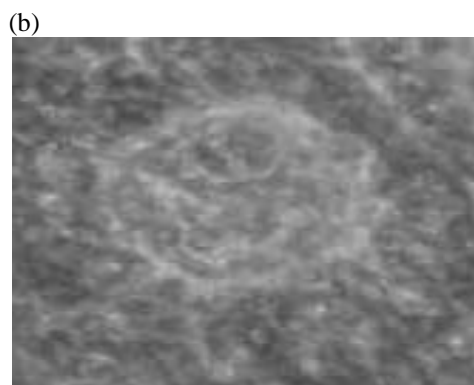
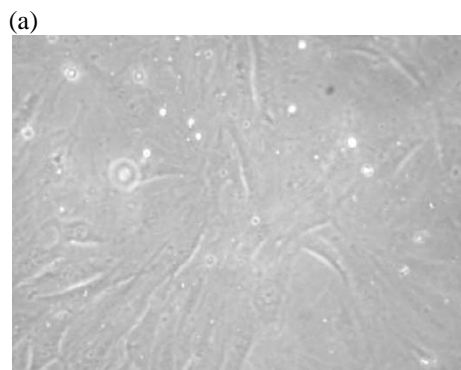
Fig 6 Graphical view of polarization with respect to height of the bi metallic electrode within the 3D hybrid micro chip

Fig 3 depicts the potential distribution with the proposed 3D micro chip where we find the non uniform distribution of potential and intra cellular organelle also effect by this field .At pole $\theta = 90^\circ$ And $\theta = 270^\circ$ the maximum potential are exposed which is similar as our numerical result. Fig 4 complete electrical potential distribution within the 3D hybrid micro chip. Where cell is affected through the whole channel. Fig 5 shows the Graphical view of electrical potential distribution with respect to height of the bi metallic electrode within the 3D hybrid micro chip. It explore that the centre part (300-600) μm of the chip holds the maximum uniform potential where the nano pores are generated at the intra organelle. Fig 6 shows the Graphical view of polarization with respect to height of the bi metallic electrode within the 3D hybrid micro chip which helps us to find out the maximum polarization area of Nono pores

5.3 Sample Preparations:

Mouse calvarias osteoblastic cells were used in this study .In order to observe only the effect of the micro devices on cells; a standard culture medium was used for all experiments. To do so, osteoblastic cells were cultivated in a standard T75 Falcon culture flask supplemented with penicillin (100 units/ml) and streptomycin (100 mg/ml), 15% fetal calf serum and with neither ascorbic acid nor beta-glycerophosphate and dexamethasone.

5.4 Observations



(c)

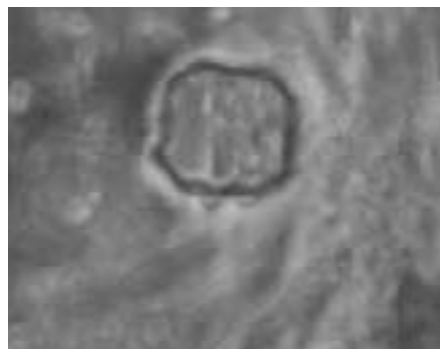


Fig: 7 Morphological views of intra organelle Nano Poration of osteoblast cell in 3D hybrid micro chip. (a) Poration osteoblast cell, (b) before intra organelle nano poration(c) after intra organelle pico poration

6. RESULTS AND DISCUSSION

Above figure shows the morphological changes of osteoblast cell. In fig 7(a) dense osteo cell. When the micro pulse is applied the cell starts to response but it is unable to penetrate the cell membrane which is exposed in fig 7(b), expected results will come when we apply the Pico pulse on the cell, a number of nano pores are generated on the intra organelle and chemicals are entered into the cell, that shows in the figure 7(C).From this observation it is exposed that there is no effect of micro pulse but pico pulse penetrate the on intraorganelle .It supports the numerical and analytical result explore in this research

This part of our study dedicated for the synchronization among the COMSOL simulation, MATLAB numerical analysis and experimental observation. As we already explore the COMSOL simulation and experimental observations so remaining contribution are completed through the graphical representation of MATLAB simulations.

Graphical representation of MATLAB simulations

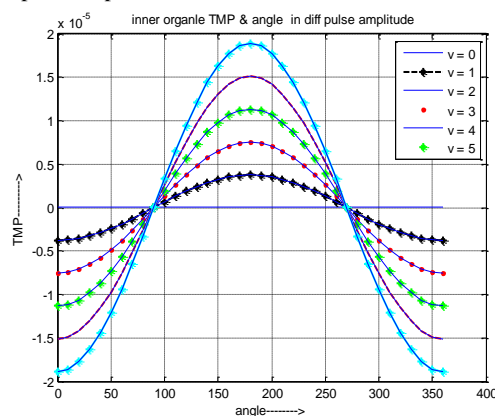


Fig. 8 .Pulse evaluation of the intra organelle membrane potential of a dense osteoblast cell located in the micro chip of height (500 μm), cell of radius a (12 μm), electrodes of width (50 μm).in a different pulse intensity

Figure 8 shows the intra organelle potential of dense osteoblast cell. For inner organelle we get the response only when the pulse intensity & width are in above picoscale range. It is exposed that pores are formed only when the pulse duration is in Pico second range and the

intra organelle potential is gradually decrease until the nanopores are generated and once the nanopores are generated, the TMP increase. The TMP has a sharper decrement at the poles ($\theta = 0$ & $\theta = 360$).The value of TMP independent of pulse duration, directly proportional pulse interval but inversely proportional with pulse intensity. As the nanopores are created, TMP increases and the angular positions of the highest TMP and the biggest nanopores move just opposite to the equator (E). In the case intra organelle potential is gradually increase until the nanopores are generated and once the nanopores are generated, the potential is reduced. It has a sharper reduction at the poles ($\theta = 180$) and its value directly proportional with value of pulse duration and intensity but inversely proportional with pulse interval. As the nanopores are created, intra organelle potential decreases and the angular positions of the highest voltage and the biggest nanopores move toward the equator (E). In all cases no voltage is obtain at the pole $\theta = 90$ & $\theta = 270$ and negative TMP is exposed during poles $\theta = 0$ to 89 & $\theta = 271$ to 360 due to the effect of rest potential. We also find out that the curve analysis of cytoplasm and nucleus are opposite in nature which reflects their reverse dielectric property and applied pulse nature provides the new information about the window effects in intra organelle of the rigid cell.

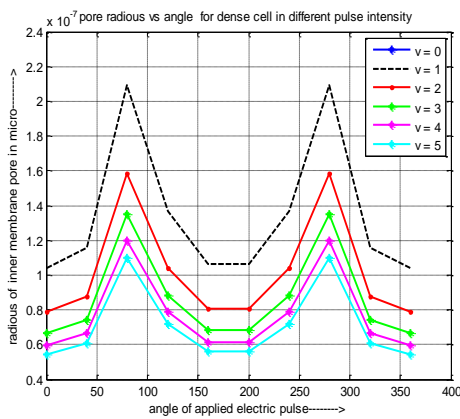


Fig 9: Pulse evaluation of the intra organelle pore radius of a dense osteoblast cell located in the micro chip of height (500µm), cell of radius a (12µm), electrodes of width (50µm), in a different pulse intensity

The above figure explores the variation of intra organelle pore radius along with pole position of applied electric field. It clears that the radius of all the pores are not same it is sinusoidal distributed over the whole surface of nucleus. The value of the pore lies in between 60 to 200 nano meter. The biggest nano pores are generated at pole $\theta = 90$ and 270 , where we get the maximum potential. As the nanopores are created, intra organelle potential increases and the biggest nanopores move just opposite to the equator (E). It is also shown that the location of the pores are as same as outer membrane and pore radius is gradually increase as the angle of applied electric field is increase & maximum pore radius is obtain at an angle of $\theta = 90$ after that it starts decrease. We also find out that the pore radius of outer membrane is greater than the radius of inner membrane of the organelle due to the higher elasticity of layers.

7. CONCLUSION

It is observed that When the micro pulse is applied the cell starts to response but it is unable to penetrate the cell membrane where as the expected results will come when we apply the Pico pulse on the cell, a number of Nano pores are generated on the intra organelle and chemicals are entered into the cell. After completion of study it is exposed that pores are formed only when the pulse duration is in Pico second range and the intra organelle potential is gradually decrease until the nanopores are generated and once the nanopores are generated, the TMP increase. The TMP has a sharper decrement at the poles ($\theta = 0$ & $\theta = 360$). When the value of TMP reaches the critical value it may cause the generation of nano pores. It clears that the radius of all the pores are not same and it is sinusoidal distributed over the whole surface of nucleus. The value of the pore lies in between 60 to 200 nano meter. The biggest nano pores are generated at pole $\theta = 90$ & $\theta = 270$, where we get the maximum potential. For pore current we get the response only when the pulse intensity & width are in above Pico scale range and the minimum pore current at pole $\theta = 90$ & 270 where organelle potential is also minimum but biggest nanopores are generated. It is also exposed that pressure is directly link with intra organelle current and both non uniformly distributed over the whole surface of the organelle. There the minimum value is exposed at pole $\theta = 90$ & 270 which is independent of pulse, electrode, micro channel and suspension media specification.

All these are related to the dielectric, elect kinetic properties of multilayer dense osteoblast cell which can also aid in understanding the basic physiological difference between normal and cancerous bone cells on a molecular level and finally all the information given in this article might provide a new light on drug delivery system and cancer treatment in bone cell. We are in process and more work has to be done to explore these possibilities.

8. ACKNOWLEDGEMENT

All of we wish to thank Dr. Soumen Das (IIT, KGP) for assistance with analytical data processing throughout the whole work.

9. REFERENCES

- [1] Andre, F., Mir, L.M., 2004. Gene Ther. 11, S33–S42.
- [2] Andre, F.M., Gehl, J., Sersa, G., Preat, V., Hojman, P., Eriksen, J., Golzio, M., Cemazar, M., Pavselj, N., Rols, M.P., Miklavcic, D., Neumann, E., Teissie, J., Mir, L.M., 2008. Hum. Gene Ther. 19 (11), 261–271.
- [3] Beebe, S.J., Schoenbach, K.H., 2005. J. Biomed. iotechnol. 4, 297–300.
- [4] Beebe, S.J., White, J., Blackmore, P.F., Deng, Y.P., Somers, K., Schoenbach, K.H., 2003. DNA Cell Biol. 22 (12), 785–796.
- [5] Berenger, J.P., 1996. J. Comput. Phys. 127 (2), 363–379.
- [6] Bowman, A.M., Nesin, O.M., Pakhomova, O.N., Pakhomov, A.G., 2010. J. Membr. Biol. 236
- [7] Buescher, E.S., Smith, R.R., Schoenbach, K.H., 2004. Plasma Sci. IEEE Trans. 32 (4), 1563–1572.

- [8] Dalmay, C., Cheray, M., Pothier, A., Lalloué, F., Jauberteau, M.O., Blondy, P., 2010. *Sens. Actuat. A: Phys.*, doi:10.1016/j.sna.2010.04.023.
- [9] El Amari, S., Kanaan, M., Merla, C., Vergne, B., Arnaud-Cormos, D., Leveque, P., Couderc, V., 2010. *Photon. Technol. Lett. IEEE* 22 (21),1577–1579.
- [10] Gothelf, A., Gehl, J., 2010. *Curr. Gene Ther.* 10 (4), 287–299.
- [11] Heller, L.C., Heller, R., 2006. *Hum. Gene Ther.* 179, 890–897.
- [12] Huang, Y., Rubinsky, B., 2001. *Sens. Actuat. A: Phys.* 89 (3), 242–249.
- [13] Ibey, B.L., Xiao, S., Schoenbach, K.H., Murphy, M.R., Pakhomov, A.G., 2009. *Bioelectromagnetics* 30 (2), 92–99.
- [14] Kanaan, M., El Amari, S., Silve, A., Merla, C., Mir, L.M., Couderc, V., Arnaud-Cormos, D., Leveque, P., 2010. *Biomed. Eng. IEEE Trans.* 58 (1), 207–214.
- [15] Krishnaswamy, P., Kuthi, A., Vernier, P.T., Gundersen, M.A., 2007. *Dielectr. Electr. Insul. IEEE Trans.* 14 (4), 871–877.
- [16] Labanauskiene, J., Gehl, J., Didziapetriene, J., 2007. *Bioelectrochemistry* 70 (1), 78–82.
- [17] Le Pioufle, B., Surbled, P., Nagai, H., Murakami, Y., Chun, K.S., Tamiya, E., Fujita, H., 2000. *Mater. Sci. Eng. C: Biomim. Supramol. Syst.* 12 (1–2), 77–81.
- [18] Lee, W.G., Demirci, U., Khademhosseini, A., 2009. *Integr. Biol.* 1 (3), 242–251. Leveque, P., Dale, C., Veyret, B., Wiart, J., 2004. *IEEE Trans. Microw. Theory Tech.* 52,(8), 2076–2083.
- [19] Leveque, P., Reineix, A., Jecko, B., 1992. *Electr. Lett.* 28 (6), 539–541.
- [20] Marty, M., Sersa, G., Garbay, J.R., Gehl, J., Collins, C.G., Snoj, M., Billard, V., Geertsen, P.F., Larkin, J.O., Miklavcic, D., Pavlovic, I., Paulin-Kosir, S.M., Cemazar, M., Morsli, N., Rudolf, Z., Robert, C., O’Sullivan, G.C., Mir, L.M., 2006. *Ejc Suppl.* 4 (11), 3–13.
- [21] Mir, L.M., Glass, L.F., Sersa, G., Teissie, J., Domenge, C., Miklavcic, D., Jaroszeski, M.J., Orłowski, S., Reintgen, D.S., Rudolf, Z., Belehradec, M., Gilbert, R., Rols, M.P., Belehradec, J., Bachaud, J.M., DeConti, R., Stabuc, B., Cemazar, M., Coninx, P., Heller, R., 1998. *Br. J. Cancer* 77 (12), 2336–2342.
- [22] Grosse, C., and H. P. Schwan. 1992. Cellular membrane potentials induced by alternating fields. *Biophys. J.* 63:1632–1642.
- [23] Kotnik, T., T. Slivnik, and D. Miklavcic. 1998. Time course of transmembrane voltage induced by time-varying electric fields: a method for theoretical analysis and its application. *Bioelectrochem. Bioenerg.* 45:3–16.
- [24] Kotnik, T., and D. Miklavcic. 2000. Second-order model of membrane electric field induced by alternating electric fields. *IEEE Trans. Biomed. Eng.* 47:1074–1081.
- [25] Kotnik, T., and D. Miklavcic. 2000. Theoretical evaluation of the distributed power dissipation in biological cells exposed to electric fields. *Bioelectromagnetics.* 21:385–394.
- [26] Foster, K. R. 2000. Thermal and non thermal mechanisms of interaction of radio-frequency energy with biological systems. *IEEE Trans. Plasma Sci.* 28:15–23.
- [27] Morse, P. M., and H. Feshbach. 1953. *Methods of Theoretical Physics.* McGraw-Hill, New York, NY
- [28] Clair Dalmay, Julien Villemejeane, et al: a microfluidic bio chip for the nanoporation of living cell. *Biosensor and Bioelectronics.* 26,12(2011) pp 4649–4655.
- [29] A Theoretical Study of Single-Cell electroporation in a Microchannel, Saïd Movahed • Dongqing Li, DOI 10.1007/s00232-012-9515-6